Choroidal Caverns in Stargardt Disease

Dario Pasquale Mucciolo,[1,2] Dario Giorgio,[1] Myrta Lippera,[1] Valeria Dattilo,[1] Ilaria Passerini,[3] Elisabetta Pelo,[3] Andrea Sodi,[1] Gianni Virgili,[1,4] Fabrizio Giansanti,[1] and Vittoria Murro[1]

[1]Department of Neuroscience, Psychology, Drug Research and Child Health, University of Florence, Florence, Italy
[2]Ophthalmology Unit, San Jacopo Hospital, Pistoia, Italy
[3]Department of Genetic Diagnosis, Careggi Teaching Hospital, Florence, Italy
[4]Fondazione GB Bietti, Roma, Italy

Correspondence: Dario Pasquale Mucciolo, Department of Neuroscience, Psychology, Drug Research and Child Health, University of Florence, Careggi Teaching Hospital, Florence Regional Reference Center for Retinal Degenerations, ERN-EYE MEMBER, Largo Brambilla, 3 - 50134 Florence, Ophthalmology Unit, San Jacopo Hospital, Pistoia, Italy, via Ciliegiole 97, 51100, Italy; dario.mucciolo@gmail.com.

Received: October 16, 2021
Accepted: January 26, 2022
Published: February 14, 2022

Citation: Mucciolo DP, Giorgio D, Lippera M, et al. Choroidal caverns in Stargardt disease. *Invest Ophthalmol Vis Sci.* 2022;63(2):25. https://doi.org/10.1167/iovs.63.2.25

Purpose. To report choroidal caverns in patients affected by recessive Stargardt disease (STGD1) and to investigate its clinical features.

Methods. Retrospective analysis of STGD1 patients recruited at the Regional Reference Center for Hereditary Retinal Degenerations at the Eye Clinic in Florence from 2012 to 2017. Patients included in the study underwent a complete ophthalmic examination including best-corrected visual acuity, color fundus photography, fundus autofluorescence, optical coherence tomography (OCT) and OCT angiography.

Results. Eighty-six patients (172 eyes) were included in the study. Twenty-three eyes (13.3%) of 21 patients presented choroidal caverns. The total number of detected choroidal caverns was 63. Choroidal caverns were only present in patients with stage III and IV STGD. Interestingly, patients with choroidal caverns presented larger macular atrophy (20.53 ± 16.9 mm^2 vs. 18.11 ± 20.39 mm^2), worse visual acuity (1.03 ± 0.29 vs. 0.83 ± 0.26), and a thinner choroidal thickness (245.9 ± 88.7 vs. 266.0 ± 110.5 µm).

Conclusions. Choroidal caverns are present only in the advanced stage of STGD1, and a possible degenerative origin of the finding has been hypothesized.

Keywords: Stargardt, choroidal caverns, OCT, STGD

Recessive Stargardt disease (STGD1) is the most common form of inherited macular dystrophy.[1] The disease is associated with pathogenic sequence variants of the *ABCA4* gene coding for a visual cycle transport protein.[2,3] Impaired function of this protein leads to the accumulation of lipofuscins and their derivatives within the retinal pigment epithelium (RPE).[4,5] STGD1 is characterized by a progressive loss of central visual function caused by the degeneration of photoreceptors and RPE cells in the macula. Recently, Querques et al.[6] described angular hyporeflective cavities called "choroidal caverns" in patients affected by geographic atrophy (GA), assuming that these findings could arise from nonperfused ghost vessels and persistence of stromal pillars where the vessels were originally situated. Dolz-Marco et al.[7] correlated a histologic survey of donor eyes with multimodal imaging from a clinical case series to demonstrate that choroidal caverns were lipid globules, suggesting that choroidal caverns might represent a common normal physiologic lipid depot for photoreceptor metabolism. Further works have expanded the prevalence of choroidal caverns in other disorders.[7–11]

Up to now, these characteristic choroidal features have rarely been investigated in patients affected by STGD1. To the authors' knowledge, only two previous studies have reported on the multimodal imaging of choroidal caverns in patients affected by STGD1[7,12]; however, no study has specifically focused on the qualitative and quantitative investigation of choroidal caverns and on their relationship with clinical outcomes in STGD1.

In the present work, we have described the choroidal caverns in a large cohort of patients affected by STGD1 evaluating the prevalence of choroidal caverns, their localization and relation with chorioretinal structures.

Materials and Methods

We retrospectively reviewed the database of patients affected by STGD1 at the Reference Center for Hereditary Retinal Degenerations at the Eye Clinic in Florence in the period from 2012 to 2017. The criteria for STGD1 diagnosis have been described in previous articles.[13] All the STGD1 patients included in the study had undergone molecular genetic testing showing at least two causative *ABCA4* mutations. Clinical phenotype was evaluated according to the Fishman classification.[14]

As part of standard clinical assessment, all patients underwent a complete ophthalmologic examination: best corrected visual acuity (BCVA), biomicroscopy of the anterior segment, measurement of intraocular pressure, and fundus examination. Color fundus photographs (FF450 Retinograph; Carl Zeiss Meditec, Jena, Germany; or Daytona,

Optos, Dunfermline, UK), fundus autofluorescence (FAF) and infrared imaging (Spectralis HRA-OCT; Heidelberg Engineering, Heidelberg, Germany) were also collected. A subset of patients also underwent OCT-angiography (OCT-A Triton; Topcon Medical Systems Inc, Oakland, NJ, USA; Spectralis HRA-OCT; Heidelberg Engineering).

OCT examinations were performed using three different OCT devices. Briefly, with SS-OCT (swept source OCT Triton; Topcon Medical Systems Inc, Oakland, NJ, USA) we used a wide scan covering a 12 × 9 mm area centered over the fovea, which comprises 256 B-scans (512 × 256 A-scans, 512 A-scans for each of the 256 B-scans) for a total of 131,072 axial scans/volume; OCT examinations using Cirrus HD-OCT (Cirrus Spectral Domain OCT, Carl Zeiss Meditec Inc.) were performed using the 512 × 128 scan pattern (macular cube protocol) where a 6 × 6 mm area on the retina centered over the fovea was scanned with 128 horizontal lines, each consisting of 512 A-scans per line (a total of 65,536 sampled points) within a scan time of 2.4 seconds; the OCT acquisition protocol using the SD-OCT (Spectralis HRA-OCT; Heidelberg Engineering) included 241 horizontal linear B-scans, each composed of 16 averaged OCT B-scans (768 A-scans per line) at 30 µm intervals, covering an area of 30° by 25° (approximately 8.5 × 7 mm^2 area) over the fovea. To achieve good visualization of the choroid, high-resolution imaging-OCT was used in all acquisitions. We used the automatic segmentation provided by the software with minor manual adjustments to ensure a correct detection of the choroidal layers when necessary. The qualitative descriptions of the collected images were performed by two retinal specialists (V.M. and D.P.M.). The same retinal specialists manually measured the choroidal thickness and the choroidal cavern greatest linear diameter. The area of atrophy was manually outlined using a caliper tool on FAF examinations in stage III and IV STGD patients (the scale of the retinal images was not adjusted for individual differences in retinal magnification because of axial length differences).

The localization of the choroidal cavern was classified according to their position in the choroid (choriocapillaris, Sattler layer and Haller layer), to the fovea (subfoveal if choroidal caverns were present <200 µm from the center of the fovea, extrafoveal if >200 µm from the center) and to the area of atrophy at the posterior pole (under the GA, outside the GA, or under the edge of the GA). The study was approved by the local Institutional Review Board (Careggi Teaching Hospital Ethics Committee) and adheres to the principles of the Helsinki Declaration.

Results

Eighty-six patients (172 eyes) from 78 independent families characterized by biallelic mutations in the *ABCA4* gene were included in the study (Table 1). Thirty-four patients were male (34/86 [39.5%]), and 52 were female. The mean age of the patients was 40.4 ± 15.6 years (range, 14–85 years) with a mean age of onset of the disease of 24.4 ± 14.0 years (range, 6–58 years). The mean BCVA (LogMar) was 0.76 ± 0.38 (range, 1.6–0) with a mean spherical equivalent of −1 ± 1.83 (range, −5.50 to 2.5). In all patients the clinical picture according to the Fishman classification was the same in both eyes: 40 eyes (40/172 [23.2%]) of 20 patients were classified as phenotype I, 30 eyes (30/172 [17.4%]) of 15 patients as phenotype II, 80 eyes (80/172; 46.5%) of 40 patients as phenotype III, and 22 eyes (22/172 [12.7%]) of 11 patients as phenotype IV.

OCT Findings

Using structural OCT, choroidal caverns were detected in 23 eyes (23/172 eyes [13.3%]) of 21 patients (bilaterally only in two patients: patients P21 and P36). The total number of choroidal caverns detected was 63. Choroidal caverns appeared as hyporeflective cavities of variable size located in the choroidal tissue. They presented a mild hyperreflective rim and a nonhomogeneous hyperreflective tail (Fig.).

The mean greatest diameter of the choroidal caverns was 67.14 ± 34.5 µm (range, 21–197 µm). In our study, 49 choroidal caverns were located in the Sattler layer and 14 in the Haller layer. No choroidal caverns were detected in the choriocapillaris. Two choroidal caverns were located in the subfoveal area whereas 61 were extrafoveal. Five choroidal caverns were visible at the edge of the macular atrophy, and 58 were located inside the area of atrophy. The mean SFCT was significantly reduced in eyes with choroidal caverns in comparison with those observed in eyes without choroidal caverns (245.1 ± 82.4 µm vs. 285.9 ± 94.3; $p = 0.05$).

OCT and Clinical Findings Correlations

The demographics and main clinical features of the study population are summarized in Tables 2A to 2C. The mean age of the patients with choroidal caverns was 47.4 ± 11.5 years (range, 23–75 years), whereas the mean age of onset of the disease was 24.7 ± 11.8 years (12–57 years). The mean BCVA was significantly lower in eyes with choroidal caverns compared to those without choroidal caverns (1.01 ± 0.29 vs. 0.81 ± 0.44; $p = 0.03$).

All eyes with choroidal caverns presented phenotype III and IV according to the Fishman classification. More precisely, of the eyes with choroidal caverns (23 eyes), 19 eyes (19/23; 82.6%) of 17 patients presented stage III and four eyes (4/23; 17.3%) of four patients presented stage IV (Table 2C).

A subgroup analysis to compare the eyes with choroidal caverns and the eyes without choroidal caverns in advanced STGD1 (stage III + stage IV, 102/172 eyes of 51 patients) did not reveal significant differences in the BCVA, SFCT, and GA extension (Table 3).

Of the eyes of patients with stage III and IV (102/172 eyes, 51 patients; 59.3%), 48 eyes of 24 patients, 28 eyes of 14 patients, and 26 eyes of 13 patients underwent DRI OCT Topcon, Cirrus HD-OCT and Spectralis HRA-OCT, respectively. Using DRI OCT Topcon we detected choroidal caverns in seven eyes (7/48, 14.5%), whereas using Cirrus HD-OCT we discovered choroidal caverns in four eyes (4/28, 14.2%). Finally, using Spectralis HRA-OCT we discovered choroidal caverns in 12 eyes (12/26 [46.1%]). In our series all the patients were examined using only one OCT device. OCTA was available for eight eyes (8/172 eyes; 4.6%) of six patients with choroidal caverns (patients P21, P23, P29, P36, P70, P81) and did not reveal any flow signal inside these lesions (Fig.).

Discussion

In this study we have reported on choroidal caverns, a characteristic finding observed in the choroid of patients affected by STGD1. Up to now, these unusual findings have been reported in patients affected by different diseases, such as atrophic age-related macular degeneration (AMD),[6,10] pachychoroid diseases,[8] and Best disease[9] and has rarely been

Table 1. Genetic Features of ABCA4 Related STGD Patients

Patient ID	*ABCA4* Mutations		Presence of Choroidal Caverns (Y/N)
P1	c.2791G>A (p.Val931Met)	c.4234C>T (p.Gln1412*)	N
P2	c.4352+1G>A (p.?)	c.6286G>A (p.Glu2096Lys)	N
P3	c.5461-10T>C p.(?)	c.5882G>A p.(Gly1961Glu)	N
P4	c.5882G>A (p.Gly1961Glu)	c.61C>T (p.Gln21*)	N
P5	c.5882G>A (p.Gly1961Glu)	c.3531C>A (p.Cys1177*)	N
P6	c.4793C>A (p.Ala1598Asp)	c.5196+2T>G (p.?)	N
P7	c.5882G>A (p.Gly1961Glu)	c.1245C>A (p.Asn415Lys)	N
P8	c.2461T>A (p.Trp821Arg)	c.5882G>A p.(Gly1961Glu)	N
P9	c.4635C>T p.(Ser1545=)	c.4640del p.(Lys1547Argfs*34)	N
P10	c.5018+2T>C p.(?)	c.6446G>T p.(Arg2149Leu)	N
P11	c.2345G>A (p.Trp782*)	c.3089T>A (p.Leu1030Gln)	N
P12	c.4667+1G>A (p.?)	c.5512C>A (p.His1838Asn)	Y
P13	c.768G>T p. = *(p.Val256Val)*	c.5714+5G>A (p.?)	Y
P14	c.5929G>A (p.Gly1977Ser)	c.5929G>A (p.Gly1977Ser)	N
P15	c.5882G>A p.(Gly1961Glu)	c.486del (p.Leu163*)	N
P16	c.1239+1G>C (p.?)	c.3296C>G (p.Ser1099*)	N
P17	c.3259G>A (p.Glu1087Lys)	c.4139C>T (p.Pro1380Leu)	N
P18	c.5198T>G (p.Met733Arg)	c.5882G>A p.(Gly1961Glu)	Y
P19	c.5018+2T>C (p.?)	c.5898+5del (p.?)	N
P20	c.5882G>A (p.Gly1961Glu)	c.4450C>T (p.Pro1484Ser)	N
P21	c.5882G>A (p.Gly1961Glu)	c.5961_5964del (p.Asp1988Profs*3)	Y
P22	c.4793C>A p.(Ala1598Asp)	c.6816+1G>A p.(?)	N
P23	c.5882G>A (p.Gly1961Glu)	c.3994_4017dup (p.Gln1332_Cys1339dup)	Y
P24	c.2069G>T (p.Gly690Val)	c.3994C>T (p.Gln1332*)	N
P25	c.5714+5G>A (p.?)	c.5917del (p.Val1973*)	N
P26	c.2791G>A (p.Val931Met)	c.3322C>T (p.Arg1108Cys)	N
P27	c.3292C>T (p.Arg1098Cys)	c.6286G>A (p.Glu2096Lys)	N
P28	c.4139C>T (p.Pro1380Leu)	c.5714+5G>A (p.?)	N
P29	c.4139C>T (p.Pro1380Leu)	c.5714+5G>A (p.?)	Y
P30	c.1846G>A (p.Glu616Lys)	c.4739T>C (p.Leu1580Ser)	N
P31	c.3364G>A (p.Glu1122Lys)	c.3364G>A (p.Glu1122Lys)	N
P32	c.634C>T p.(Arg212Cys)	c.634C>T p.(Arg212Cys)	N
P33	c.5087G>A (p.Ser1696Asn)	c.6288G>T (p.Glu2096Asp)	N
P34	c.3610G>A (p.Asp1204Asn)	c.5527C>T (p.Arg1843Trp)	N
P35	c.2888G>T (p.Gly963Val)	c.6449G>A (p.Cys2150Tyr)	N
P36	c.2300T>A (p.Val767Asp)	c.3584_3585insGT (p.Thr1196*)	Y
P37	c.5882G>A (p.Gly1961Glu)	c.6658C>T (p.Gln2220*)	N
P38	c.5882G>A (p.Gly1961Glu)	c.3056C>T (p.T1hr019Met)	N
P39	c.982G>T (p.Glu328*)	c.2828G>A (p.Arg943Gln)	Y
P40	c.5882G>A (p.Gly1961Glu)	c.2791G>A (p.Val931Met)	N
P41	c.2791G>A (p.Val931Met)	c.4234C>T (p.Gln1412*)	Y
P42	c.5381C>A (p.Ala1794Asp)	c.6072_6074del (p.Asp2024del)	Y
P43	c.1714C>T (p.Arg572*)	c.4417C>A (p.Leu1473Met)	N
P44	c.5917del p.(Val1973*)	c.5917del p.(Val1973*)	N
P45	c.247_250dup p.(Ser84Thrfs*16)	c.286A>G p.(Asn96Asp)	N
P46	c.1622T>C (p.Leu541Pro)	c.3113C>T (p.Ala1038Val)	Y
P47	c.5882G>A (p.Gly1961Glu)	c.3261A>C (p.Glu1087Asp)	N
P48	c.667A>C (p.Lys223Gln)	c.3212C>T (p.Ser1071Leu)	Y
P49	c.634C>T (p.Arg212Cys)	c.3806T>C (p.Leu1269Pro)	Y
P50	c.5882G>A (p.Gly1961Glu)	c.6416G>T (p.Arg2139Leu)	N
P51	c.247_250dup (p.Ser84Thrfs*16)	c.1666A>G (p.Met556Val)	N
P52	c.61C>T (p.Gln21*)	c.2774G>A (p.Trp925*)	N
P53	c.5882G>A (p.Gly1961Glu)	c.5425_5426del (p.Ile1809Tyrfs*8)	N
P54	c.5882G>A (p.Gly1961Glu)	c.5917del (p.Val1973*)	N
P55	c.5917del (p.Val1973*)	c.5917del (p.Val1973*)	N
P56	c.5882G>A p.(Gly1961Glu)	c.5018+2T>C (p.?)	N
P57	c.5882G>A (p.Gly1961Glu)	c.514G>A (p.Gly172Ser)	N
P58	c.5882G>A (p.Gly1961Glu)	c.5018+2T>C (p.?)	N
P59	c.1957C>T (p.Arg653Cys)	c.6721C>G (p.Leu2241Val)	N
P60	c.2461T>A (p.Trp821Arg)	c.3323G>A (p.Arg1108His)	N
P61	c.5882G>A (p.Gly1961Glu)	c.6445C>T (p.Arg2149*)	N
P62	c.1A>G (p.Met1Val)	c.868C>T (p.Arg290Trp)	N
P63	c.3323G>A (p.Arg1108His)	c.5882G>A (p.Gly1961Glu)	N
P64	c.286A>G (p.Asn96Asp)	c.5882G>A (p.Gly1961Glu)	N

Investigative Ophthalmology & Visual Science

Table 1. Continued

Patient ID	*ABCA4* Mutations		Presence of Choroidal Caverns (Y/N)
P65	c.2640G>C (p.Thr880Cys)	c.2640G>C (p.Thr880Cys)	N
P66	c.3292C>T (p.Arg1098Cys)	c.6479+3A>C (p.?)	N
P67	c.1140T>A (p.Asn380Lys)	c.5882G>A (p.Gly1961Glu)	Y
P68	c.5413A>G (p.Asn1805Asp)	c.5714+5G>A (p.?)	Y
P69	c.288C>A (p.Asn96Lys)	c.2791G>A (p.Val931Met)	N
P70	c.5882G>A (p.Gly1961Glu)	c.571-2A>T (p.?)	Y
P71	c.571-2A>T (p.?)	c.2743G>A (p.Asp915Asn)	N
P72	c.2774G>A (p.Trp925*)	c.6449G>A (p.Cys2150Tyr)	N
P73	c.4919G>A (p.Arg1640Glu)	c.6446G>T (p.Arg2149Leu)	Y
P74	c.4667+1G>A (p.?)	c.5882G>A (p.Gly1961Glu)	N
P75	c.1622T>C (p.Leu541Pro)	c.3113C>T (p.Ala1038Val)	Y
P76	c.1622T>C (p.Leu541Pro)	c.3113C>T (p.Ala1038Val)	N
P77	c.2099G>A (p.Trp700*)	c.5882G>A (p.Gly1961Glu)	N
P78	c.286A>C (p.Asn96His)	c.5882G>A (p.Gly1961Glu)	Y
P79	c.2345T>A (p.Trp782*)	c.3089T>A (p.Leu1030Gln)	N
P80	c.5819T>A (p.Leu1940Gln)	c.5882G>A (p.Gly1961Glu)	Y
P81	c.1622T>C (p.Leu541Pro)	c.3113C>T (p.Ala1038Val)	Y
P82	c.3056C>T (p.Thr1019Met)	c.6446G>T (p.Arg2149Leu)	N
P83	c.4793C>A (p.Ala1598Asp)	c.5196+2T>G (p.?)	N
P84	c.5882G>A p.(Gly1961Glu)	c.5929G>A (p.Gly1977Ser)	N
P85	c.982G>T (p.Glu328*)	c.5882G>A (p.Gly1961Glu)	N
P86	c.5882G>A (p.Gly1961Glu)	c.3933G>A (p.Gly978Asp)	N

Y: yes; N: no.

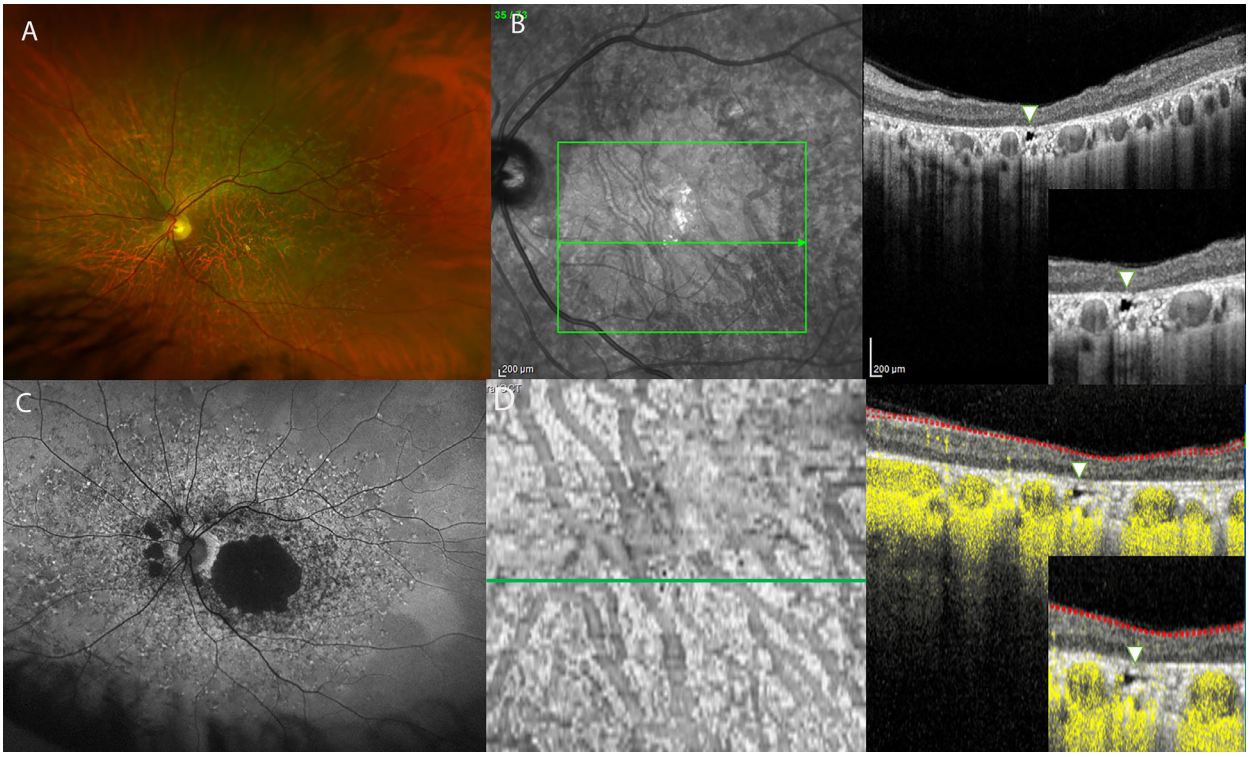

Figure. (**A**) Wide-field color fundus photograph of the left eye of a patient affected by STGD1. (**B**) OCT scan showing choroidal caverns (*arrowhead*). (**C**) Fundus autofluorescence imaging characterized by a wide central hypoautofluorescent area surrounded by a speckled FAF response. (**D**) OCT-A examination does not reveal any flow signal inside the choroidal cavern lesion.

reported in patients affected by STGD1.[7,12] The prevalence of choroidal caverns varied in literature: 12.5% and 42% in eyes affected by GA,[6,10] and 52% in eyes affected by pachychoroid disease.[8] In our study, we have reported a mean prevalence of 13.3% for choroidal caverns (23/172 eyes of 21 patients) in STGD1. However, we should take into

Investigative Ophthalmology & Visual Science

Table 2A. Demographics of the Study Population

	With Choroidal Caverns	With No Choroidal Caverns	*p* Value
Number of eyes	23	149	
Sex M (n patients)	6 M – 15F	28 M – 37F	
Age (yrs.)	47.4 ± 11.5	38.2 ± 16.1	0.01
Age of onset (y)	24.7 ± 11.8	24.3 ± 14.6	0.91
Disease duration (y)	22.1 ± 8.3	13.8 ± 9.3	<0.001
BCVA (Log Mar)	1.01 ± 0.29	0.81 ± 0.44	0.03
SFCT (micron)	245.1 ± 82.4	285.9 ± 94.3	0.05

Table 2B. Main Clinical Features of the Study Population: Choroidal Caverns Features (n = 63)

Mean Diameter (µm)	**67.14 ± 34.5**
Subfoveal/Extrafoveal (n)	2/61
Edge atrophy/Inside atrophy (n)	5/58
Haller layer/Sattler layer (n)	14/49
Mean diameter (µm)	67.14 ± 34.5

Table 2C. Main Clinical Features of the Study Population: Eyes With and Without Choroidal Caverns Stratified According to the Clinical Phenotype Fishman Classification

	No. of Eyes With Choroidal Caverns	No. of Eyes Without Choroidal Caverns
Stage I	0	40
Stage II	0	30
Stage III	19	61
Stage IV	4	18

Table 3. Demographic and Clinical Features of Stage III and IV STGD Patients

	With Choroidal Caverns	Without Choroidal Caverns	*p* Value
Number of eyes	23	79	
Sex (no. of patients)	6 M/15 F	13 M/17 F	
Age (y)	47.4 ± 11.5	42.0 ± 17.1	0.20
Age of onset (y)	24.7 ± 11.8	23.4 ± 16.3	0.77
Disease duration (y)	22.1 ± 8.3	17.9 ± 9.5	0.12
BCVA (Log Mar)	1.01 ± 0.29	1.03 ± 0.32	0.74
SFCT (µm)	245.1 ± 82.4	261.4 ± 107.3	0.50
GA (mm^2)	20.46 ± 15.6	18.89 ± 19.8	0.74

GA, geographic atrophy.

consideration that the prevalence of the choroidal caverns could be partially influenced because of the use of different OCT devices and, of course, of the different acquisition protocol.[6,8,10,12] An OCT denser coverage acquisition protocol could result in a higher detection rate for this unusual finding.

From a morphological point of view, the choroidal caverns appeared as well-defined cavities of variable shape and size. The central part of these cavities is darker compared to the background, and all the choroidal caverns showed a mild hyperreflective rim and had a characteristic hypertransmission tail. With respect to the size, several studies reported variable results: a mean size of 115 µm and 67.7 µm have been described in atrophic AMD patients[6,10]; Dolz-Marco et al.[7] demonstrated a cavern size of 61 µm, whereas eyes affected by pachychoroid disease tended to have a larger maximum size, ranging from 249 to 486 µm.[8] In our study, we have reported a mean diameter of 67.14 ± 34.5 µm, which is in line with the results previously reported for patients affected by GA.[10] Morphological similarities (size, diameter) and prevalence data between the choroidal caverns reported in this study and the choroidal caverns previously reported in literature could suggest a possible common etiopathogenetic origin for these rare choroidal features for AMD and STGD1 patients. More specifically, we know that the exact origin and pathogenetic mechanism of this peculiar finding is not clear[6,7,8]; however, in STGD1, the development of choroidal caverns could be directly related to the process of RPE impairment and atrophy: first, we observed choroidal caverns only in eyes affected by stage III and IV STGD1 (more advanced stages); second, choroidal caverns were found in areas of the choroid underneath RPE atrophy, localized in both the Sattler and Haller layer, and no choroidal caverns were discovered in the choriocapillaris (CC) layer; third, no choroidal caverns were discovered outside the area of macular atrophy or in the surrounding retina. We know that the health of the RPE is crucial for choroid architecture development whereas RPE impairment causes progressive choroidal sclerosis.[4] The RPE secretes a variety of growth factors, and an increasing body of evidence indicates that RPE-derived trophic factors are essential for normal choroidal development.[15,16] Choroidal caverns appear as empty structures characterized by the absence of any pathological blood flow detectable using OCTA; for this reason, the focal obliteration of some choroidal vessels may be a possible explanation for the development of choroidal caverns in STGD1; however, we cannot definitely exclude that choroidal caverns may correspond to tiny vessels characterized by a slow flow which is not detectable using OCTA. For all these reasons we suggest that the RPE impairment observed in the STGD1 patients, more evident in stage III and IV, could be responsible for the development of the choroidal caverns.

We have also investigated the association between choroidal caverns and some clinical features of the disease, such as SFCT, BCVA, and the extension of macular atrophy, the latter was measured only in stage III and IV STGD1 patients.

Up to now, several articles have taken into consideration the association between different OCT parameters and specific features of STGD1. SFCT has been found to be positively associated with a better BCVA and a higher foveal thickness and inversely related to duration of the disease, severe fundus alterations, and electroretinogram (ERG) abnormalities.[13] Vural et al.[17] recently reported a statistically significant correlation between subfoveal SFCT and BCVA, inner and outer retinal thickness and paracentral multifocal electroretinogram (mf-ERG) responses, whereas Arrigo et al.[12] reported that STGD1 eyes with choroidal caverns were associated with lower BCVA, retinal layer thinning, and higher hyperreflective foci numbers.

In our study, we observed that patients with choroidal caverns presented a thinner choroid and worse visual acuity in comparison with patients without choroidal caverns, and these differences are significant. However, this result may be partially due to the more advanced stage of disease (stage III and IV) that characterized all patients with choroidal caverns in comparison with patients without; in fact, from past studies we know that both the BCVA and SFCT have been found to be inversely related to duration of the disease and more severe fundus alterations.[12,13]

For this reason, we took into consideration only patients with more advanced disease stages (stage III and IV) and excluded patients with stage I and II, and we compared the patients with and without choroidal caverns: we did not detect differences in either the BCVA or the SFCT. Further-

more, no differences were detected in the GA area extension in these two study groups. Therefore the BCVA, SFCT, and GA area extension did not differ between eyes with and without choroidal caverns in the more advanced stages of the disease; we could not identify and clarify the prognostic role of choroidal caverns in STGD1 patients. Future studies are necessary to better highlight the role of choroidal caverns in STGD1.

Finally, in our work we have evaluated possible genotype-phenotype correlation between specific genetic variants of the *ABCA4* gene and the presence of choroidal caverns. However, we are unable to show a genotype/phenotype association between specific genetic variants and the presence of choroidal caverns in our cohort.

We are aware of some limitations of our study, which include its retrospective nature, the lack of histological data of the choroidal caverns, and the use of different OCT devices; however, we studied in detail a large number of genetically characterized patients.

In conclusion, we identified choroidal caverns in STGD1 as hyporeflective cavities of variable size characterized by the absence of flow using OCTA; we found similar morphological and prevalence data with the choroidal caverns previously reported in AMD; the choroidal caverns are present only in advanced stages of STGD1, suggesting a degenerative origin caused by the RPE impairment, more evident in stage III and IV of the disease.

Acknowledgments

Disclosure: **D.P. Mucciolo,** None; **D. Giorgio,** None; **M. Lippera,** None; **V. Dattilo,** None; **I. Passerini,** None; **E. Pelo,** None; **A. Sodi,** None; **G. Virgili,** None; **F. Giansanti,** None; **V. Murro,** None

References

1. Cornish KS, Ho J, Downes S, Scott NW, Bainbridge J, Lois N. The epidemiology of Stargardt disease in the United Kingdom. *Ophthalmol Retina*. 2017;1:508–513.
2. Allikmets R, Singh N, Sun H, et al. A photoreceptor cell-specific ATP-binding transporter gene (ABCR) is mutated in recessive Stargardt macular dystrophy. *Nat Genet*. 1997;15:236–246.
3. Passerini I, Sodi A, Giambene B, Mariottini A, Menchini U, Torricelli F. Novel mutations in of the ABCR gene in Italian patients with Stargardt disease. *Eye Lond Engl*. 2010;24:158–164.
4. Cideciyan AV, Aleman TS, Swider M, et al. Mutations in ABCA4 result in accumulation of lipofuscin before slowing of the retinoid cycle: a reappraisal of the human disease sequence. *Hum Mol Genet*. 2004;13:525–534.
5. Radu RA, Yuan Q, Hu J, et al. Accelerated accumulation of lipofuscin pigments in the RPE of a mouse model for ABCA4-mediated retinal dystrophies following vitamin A supplementation. *Invest Ophthalmol Vis Sci*. 2008;49:3821–3829.
6. Querques G, Costanzo E, Miere A, Capuano V, Souied EH. Choroidal caverns: a novel optical coherence tomography finding in geographic atrophy. *Invest Ophthalmol Vis Sci*. 2016;57:2578–2582.
7. Dolz-Marco R, Glover JP, Gal-Or O, et al. Choroidal and subretinal pigment epithelium caverns: multimodal imaging and correspondence with Friedman lipid globules. *Ophthalmology*. 2018;125:1287–1301.
8. Sakurada Y, Leong BCS, Parikh R, Fragiotta S, Freund KB. Association between choroidal caverns and choroidal vascular hyperpermeability in eyes with pachychoroid diseases. *Retina Phila Pa*. 2018;38:1977–1983.
9. Carnevali A, Sacconi R, Corbelli E, Querques L, Bandello F, Querques G. Choroidal caverns: a previously unreported optical coherence tomography finding in best vitelliform dystrophy. *Ophthalmic Surg Lasers Imaging Retina*. 2018;49:284–287.
10. Corbelli E, Sacconi R, De Vitis LA, et al. Choroidal round hyporeflectivities in geographic atrophy. *PloS One*. 2016;11(11):e0166968.
11. Sun LW, Johnson RD, Williams V, et al. Multimodal imaging of photoreceptor structure in choroideremia. *PLoS One*. 2016;11(12):e0167526.
12. Arrigo A, Grazioli A, Romano F, et al. Choroidal Patterns in Stargardt Disease: Correlations with Visual Acuity and Disease Progression. *J Clin Med*. 2019;8(9):1388.
13. Sodi A, Bacherini D, Lenzetti C, et al. EDI OCT evaluation of choroidal thickness in Stargardt disease. *PloS One*. 2018;13(1):e0190780.
14. Fishman GA. Fundus flavimaculatus. A clinical classification. *Arch Ophthalmol Chic Ill 1960*. 1976;94:2061–2067.
15. Saint-Geniez M, Maldonado AE, D'Amore PA. VEGF expression and receptor activation in the choroid during development and in the adult. *Invest Ophthalmol Vis Sci*. 2006;47:3135–3142.
16. Saint-Geniez M, Kurihara T, Sekiyama E, Maldonado AE, D'Amore PA. An essential role for RPE-derived soluble VEGF in the maintenance of the choriocapillaris. *Proc Natl Acad Sci USA*. 2009;106:18751–18756.
17. Vural E, Acar U, Sevinc MK, et al. Choroidal thickness in patients with Stargardt disease. *Retina*. 2018;38:614–619.